
Denoising Noisy Neural Networks: A Bayesian Approach with Compensation

Yulin Shao*

Department of Electrical and Electronic Engineering
Imperial College London
London SW7 2AZ, U.K.
y.shao@imperial.ac.uk

Soung Chang Liew

Department of Information Engineering
The Chinese University of Hong Kong
Shatin, NT, Hong Kong
soung@ie.cuhk.edu.hk

Deniz Gündüz

Department of Electrical and Electronic Engineering
Imperial College London
London SW7 2AZ, U.K.
d.gunduz@imperial.ac.uk

Abstract

Noisy neural networks (NoisyNNs) refer to the inference and training of NNs in the presence of noise. Noise is inherent in most communication and storage systems; hence, NoisyNNs emerge in many new applications, including federated edge learning, where wireless devices collaboratively train a NN over a noisy wireless channel, or when NNs are implemented/stored in an analog storage medium. This paper studies a fundamental problem of NoisyNNs: how to estimate the uncontaminated NN weights from their noisy observations or manifestations. Whereas all prior works relied on the maximum likelihood (ML) estimation to maximize the likelihood function of the estimated NN weights, this paper demonstrates that the ML estimator is in general suboptimal. To overcome the suboptimality of the conventional ML estimator, we put forth an MMSE_{pb} estimator to minimize a compensated mean squared error (MSE) with a population compensator and a bias compensator. Our approach works well for NoisyNNs arising in both 1) noisy inference, where noise is introduced only in the inference phase on the already-trained NN weights; and 2) noisy training, where noise is introduced over the course of training. Extensive experiments on the CIFAR-10 and SST-2 datasets with different NN architectures verify the significant performance gains of the MMSE_{pb} estimator over the ML estimator when used to denoise the NoisyNN. For noisy inference, the average gains are up to 156% for a noisy ResNet34 model and 14.7% for a noisy BERT model; for noisy training, the average gains are up to 18.1 dB for a noisy ResNet18 model.

1 Introduction

Noise is inherent in all communication and storage systems. When the parameters of neural networks are communicated over a wireless channel or stored in a non-ideal medium, the parameters will be contaminated with noise, giving rise to noisy neural networks (NoisyNNs). For example, federated edge learning (FEEL) with over-the-air computation (OAC) [1–3] leads to NoisyNNs. FEEL is a distributed/federated learning algorithm, where multiple edge devices that share the same wireless

*Y. Shao was with the Department of Information Engineering, The Chinese University of Hong Kong.

medium collaboratively train a common model [4, 5]. Orchestrated by a base station (BS), FEEL proceeds in an iterative manner; at each iteration, the edge devices update the NN model locally using their private data, and transmit their local model updates (e.g., the gradients) back to the BS for aggregation via OAC. In particular, devices transmit their local updates in an uncoded and synchronized manner so that they coherently arrive at the BS, which receives the summation of the transmitted updates thanks to signal superposition property of the wireless medium. In this process, additive white Gaussian noise (AWGN) is also introduced by the wireless channel; and hence, the aggregated NN model at the BS is a NoisyNN.

The deployment of NN on analog hardware [6–10] also produces NoisyNNs. In this application, the computations inside a NN are executed in the analog domain with digital weights being represented by analog quantities, e.g., conductance [6], electrical voltages [9], or photons [10]. Compared with digital hardware, analog hardware promises at least two orders of magnitude greater gains in both computational speed and energy efficiency [6, 8, 10]. Analog quantities, however, are subject to thermal noise generated by their physical components – often the deployed weights are different from the expected weights on an analog device. In other words, analog computations are inherently noisy and the deployed neural networks are NoisyNNs. In particular, the noise in analog hardware is often modeled as AWGN to mimic the overall effect of many concurrent random effects. The efficient storage of NN weights in analog hardware, on the other hand, faces the same problem: the retrieved NN from an analog device is a noisy version of the stored NN [11], due to the noisy nature of analog hardware.

In addition to the above analog communication and storage scenarios, in conventional digital systems, the precision loss of NN weights due to quantization [12] and truncation [13] can also be viewed as a kind of noise. Although this kind of noise is deterministic, it is shown to behave like Gaussian noise in the high-rate compression regime for various types of quantization and compression schemes [14–16], implying that the average estimation error achieved when the compressed representation of data is available is asymptotically equivalent to the one achieved from a Gaussian-noise corrupted version.

A fundamental problem of NoisyNN is how to denoise the noisy NN weights. All previous works [1–3, 6–11, 17–20] take the noisy observations/manifestations directly as the estimated NN weights. In the language of statistical inference, this is essentially the maximum likelihood (ML) estimation since the raw observations maximize the likelihood function of the true NN weights under AWGN.

This paper, however, demonstrates that the ML estimation is in general suboptimal in terms of maximizing the inference accuracy of the estimated NN model. By exploiting the statistical characteristics of the NN weights as a kind of prior information, we put forth a Bayesian compensated minimum mean squared error (MMSE) estimator. Specifically, a “population compensator” and a “bias compensator” are introduced in the MMSE estimation method and we refer to the resulting estimator as the MMSE_{pb} estimator. Two main ingredients of the MMSE_{pb} estimator are Bayesian estimation and compensators for Bayesian estimation:

1. **Bayesian estimation.** Instead of ML estimation, we assume the true NN weights are generated from a statistical model and perform Bayesian estimation to minimize the MSE or maximize the *a posteriori* probability (MAP). Given the complex architecture of today’s NNs, acquiring the true statistical model is elusive. Thus, we approximate the statistical model by a Gaussian prior – which is parameterized by the sample mean and sample variance of the true NN weights – and assume that the NN weights are sampled from the approximated Gaussian in an independently and identically distributed (i.i.d.) manner. In so doing, an MMSE estimator is devised to minimize the MSE between the estimated weights and the true weights (note that the MMSE estimator is also a MAP estimator since both criteria are equivalent under the assumption of a Gaussian prior).
2. **Compensators for Bayesian estimation.** An MMSE estimator minimizes the MSE for the estimated NN weights but does not necessarily maximize the inference accuracy of the estimated model. This is because the NN weight with a larger magnitude matters more than that with a smaller magnitude as far as the inference accuracy is concerned, while the MMSE metric, on the other hand, treats each NN weight equally. In this light, we put forth a population compensator and a bias compensator to the MMSE metric and devise an MMSE_{pb} estimator to denoise the noisy NN weights.

Extensive experimental results on the CIFAR-10 [21] and SST-2 [22] datasets with different NN architectures verify the superior performance of the MMSE_{pb} estimator over the ML estimator. In particular, we consider two classes of NoisyNNs, where noise is introduced in the inference phase and the training phase, respectively.

1. **Noisy inference.** We consider three well-trained NN models (ResNet34 [23], ResNet18 [23], and ShuffleNet V2 [24]) for the CIFAR-10 task and a BERT model [25] for the SST-2 task. We generate NoisyNNs by adding AWGN noise to the already-trained NN weights according to a given signal-to-noise ratio (SNR). When our MMSE_{pb} estimator is used to denoise the NNs, the average test-accuracy gains over the ML estimator are up to 156%, 85%, 21%, and 14.7% on the ResNet34, ResNet18, ShuffleNet V2, and BERT, respectively.
2. **Noisy training.** In the application of FEEL with OAC, noise is introduced in the training phase in each FEEL iteration. When using our MMSE_{pb} estimator at the receiver to estimate the aggregated model, remarkable gains over the ML estimator are observed. For the ShuffleNet V2 model, the average test-accuracy gains are up to 59.1%. For the ResNet18 model, the test-accuracy gains boost significantly: to achieve a test accuracy of 60%, the MMSE_{pb} estimator is 18.1 dB better than the ML estimator in terms of SNR; to achieve a test accuracy of 80%, the MMSE_{pb} estimator is 11.3 dB better than the ML estimator.

Notations: Throughout the paper, we use boldface lowercase letters (e.g., \mathbf{x} , \mathbf{w}) to denote column vectors; the cardinality of a vector \mathbf{w} is denoted by $|\mathbf{w}|$; $\mathbf{I}_{d \times d}$ is a d -dimensional identity matrix; \mathbb{R} stands for the set of real numbers; \mathcal{N} stands for the real Gaussian distribution.

2 System Model

2.1 Noisy neural networks (NoisyNN)

We consider an artificial neural network \mathcal{F} with input vector $\mathbf{x} \in \mathbb{R}^{d_x}$, output vector $\mathbf{y} \in \mathbb{R}^{d_y}$, and parameter vector $\mathbf{w} \in \mathbb{R}^d$: $\mathbf{y} = \mathcal{F}(\mathbf{x}|\mathbf{w})$. Given a collection of N training examples $\{\mathbf{x}^n, \mathbf{y}^n : n = 1, 2, 3, \dots, N\}$, the goal is to identify the parameter vector \mathbf{w} that minimizes a specified loss function $\mathcal{L}(\{\mathbf{x}^n, \mathbf{y}^n\}, \mathbf{w})$. The machine learning process can be broken into two phases:

1. **The training phase.** The training phase typically proceeds over multiple epochs. In the i -th epoch, the parameter vector $\mathbf{w}^{(i)}$ is updated via the back-propagation algorithm in the negative gradient direction:

$$\mathbf{w}^{(i+1)} = \mathbf{w}^{(i)} - \text{lr}^{(i)} \times \nabla_{\mathbf{w}^{(i)}} \mathcal{L}(\{\mathbf{x}^n, \mathbf{y}^n\}, \mathbf{w}^{(i)}), \quad (1)$$

where $\text{lr}^{(i)}$ is the learning rate scaling the magnitude of the gradients. As the training progresses, the updated \mathbf{w} yields smaller and smaller training loss.

2. **The inference/deployment phase.** When the training phase is complete, the trained parameter vector \mathbf{w}^* that minimizes the loss function over the training data set is then deployed to make predictions on unseen data samples.

In practical systems, the parameters \mathbf{w} can be exposed to noise in either the training phase, the inference phase, or both. In general, the observed parameter vector $\mathbf{r} \in \mathbb{R}^d$ is a noisy version of the true vector:

$$\mathbf{r} = \mathbf{w} + \mathbf{z}, \quad (2)$$

where the noise term \mathbf{z} can often be modeled as AWGN. That is, the elements of \mathbf{w} are sampled from a Gaussian random variable $Z \sim \mathcal{N}(Z; 0, \sigma_z^2)$ in an i.i.d. manner. With noisy weights, the NN becomes a NoisyNN. In particular, the noise power/variance σ_z^2 is not controllable, and hence, such noise is often detrimental to network training and inference.

Remark 1. *Noise is not always detrimental to learning. Under proper management, noise can also be beneficial. In deep reinforcement learning [26], for example, adding parametric noise (i.e., noise with learnable mean and variance) to the weights of a policy network enhances exploration. Furthermore, deliberately added training noise has a regularization effect that prevents the NN from overfitting [27].*

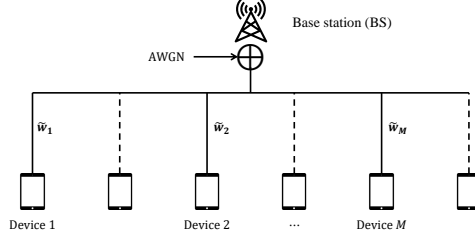


Figure 1: In FEEL with OAC, multiple edge devices collaboratively train a common model with the help of a BS. The uplink model aggregation is realized by OAC.

2.2 Federated edge learning (FEEL)

In FEEL, a number of edge devices collaboratively train a shared model with the help of a BS, as shown in Fig. 1. Data are distributed at the edge devices and cannot be shared among devices due to privacy concerns. The edge devices train the NN locally using their local data and transmit the model updates to the BS with OAC. One iteration of FEEL operates as follows:

1. Downlink broadcast. The BS maintains a global NN model $\mathbf{w}_0 \in \mathbb{R}^d$ and periodically broadcasts the latest model to the edge devices at the beginning of an iteration.
2. Local training. Upon receiving the latest global model, a subset of devices, which are willing to participate in the training in this iteration, train the global model locally using their private dataset for one or more epochs. Let there be M devices participating in the training. Each of the M devices obtains a new model $\mathbf{w}_m \in \mathbb{R}^d$, $m = 1, 2, 3, \dots, M$, after training.
3. OAC. The M devices transmit their model updates $\tilde{\mathbf{w}}_m = \mathbf{w}_m - \mathbf{w}_0$ simultaneously to the BS in an analog fashion.² The signals from different devices overlap at the BS and yield

$$\mathbf{r} = \sum_{m=1}^M \tilde{\mathbf{w}}_m + \mathbf{z} \triangleq \mathbf{w} + \mathbf{z}, \quad (3)$$

thanks to the superposition nature of the uplink multiple-access channel (MAC). In particular, \mathbf{z} is AWGN with a power spectrum density σ_z^2 .

4. Given the received vector \mathbf{r} , the BS estimates the arithmetic sum of the model updates $\mathbf{w} = \sum_{m=1}^M \tilde{\mathbf{w}}_m$ and updates the global model by $\mathbf{w}_0 = \mathbf{w}_0 + \frac{1}{M}\mathbf{w}$.

As can be seen, the edge devices and the BS have to exchange the NN weights wirelessly over a number of training iterations. In each iteration, AWGN is introduced by the uplink wireless channel and the updated global model \mathbf{w}_0 is a NoisyNN. When the received SNR in (3) is low, the noise can hinder the convergence of FEEL.

3 Bayesian Estimation with Compensators

3.1 ML estimation

A fundamental problem in the NoisyNN is how to estimate the uncontaminated NN weights \mathbf{w} from their noisy observations/manifestations \mathbf{r} . All previous works [1–3, 6–11, 17–20] take the raw observation \mathbf{r} as the estimate of \mathbf{w} . This is essentially an ML estimator given in Definition 1.

Definition 1 (ML estimation). *Given the observed NN weight vector $\mathbf{r} \in \mathbb{R}^d$ in (2), the ML estimate of the uncontaminated weight vector \mathbf{w} is*

$$\hat{\mathbf{w}}^{ML} = \mathbf{r}. \quad (4)$$

²In fading channels, an additional step before the analog transmission is the channel-coefficient precoding. That is, each device precodes the model updates $\tilde{\mathbf{w}}_m$ by the inversion of the uplink channel coefficients to pre-compensate the channel distortion. By doing so, the fading MAC degenerates to a Gaussian MAC, as in (3).

The reason behind (4) is as follows. In ML estimation, the real NN weight \mathbf{w} is treated as a constant vector. The likelihood function $p(\mathbf{r}|\mathbf{w})$ is then a d -dimensional Gaussian $p(\mathbf{r}|\mathbf{w}) \sim \mathcal{N}(\mathbf{w}; \mathbf{r}, \Sigma_z)$, where the covariance matrix Σ_z is a diagonal matrix since the elements of \mathbf{z} are i.i.d. Gaussian noise. Therefore, the ML estimate of \mathbf{w} is the mean of $p(\mathbf{r}|\mathbf{w})$, which gives us $\hat{\mathbf{w}}^{\text{ML}}$.

In this work, we ask the following question: is it possible to do better than ML estimation? This section answers this question affirmatively by putting forth a Bayesian estimator with a population compensator and a bias compensator.

3.2 Bayesian estimation

To start with, let us consider the Bayesian estimation of \mathbf{w} . ML estimation treats \mathbf{w} as a constant vector and aims to find the ML estimate $\hat{\mathbf{w}}^{\text{ML}}$. Bayesian estimation, on the other hand, treats \mathbf{w} as a random vector sampled from a statistical model $p(\mathbf{w})$ and aims to find either the MMSE estimate $\hat{\mathbf{w}}^{\text{MMSE}}$ or the maximum *a posteriori* (MAP) estimate $\hat{\mathbf{w}}^{\text{MAP}}$. Specifically, the MMSE estimate $\hat{\mathbf{w}}^{\text{MMSE}}$ minimizes the MSE:

$$\begin{aligned} \hat{\mathbf{w}}^{\text{MMSE}} &= \min_{\hat{\mathbf{w}}} \mathbb{E} \left[(\hat{\mathbf{w}} - \mathbf{w})^2 | \mathbf{r} \right] = \min_{\hat{\mathbf{w}}} \int (\hat{\mathbf{w}} - \mathbf{w})^2 p(\mathbf{w}, \mathbf{r}) d\mathbf{w} \\ &\propto \min_{\hat{\mathbf{w}}} \int (\hat{\mathbf{w}} - \mathbf{w})^2 p(\mathbf{r}|\mathbf{w}) p(\mathbf{w}) d\mathbf{w}, \end{aligned} \quad (5)$$

while the MAP estimate $\hat{\mathbf{w}}^{\text{MAP}}$ maximizes the posterior probability:

$$\hat{\mathbf{w}}^{\text{MAP}} = \max_{\mathbf{w}} p(\mathbf{w}|\mathbf{r}) \propto p(\mathbf{r}|\mathbf{w}) p(\mathbf{w}). \quad (6)$$

The likelihood function $p(\mathbf{r}|\mathbf{w})$ in (5) and (6) is determined by the channel model (2). Thus, we have $p(\mathbf{r}|\mathbf{w}) \sim \mathcal{N}(\mathbf{w}; \mathbf{r}, \Sigma_z)$, as in the ML estimation. The joint distribution of the NN weights $p(\mathbf{w})$, on the other hand, describes the interrelationships among the NN weights and is unlikely to be known to the observer/receiver. This suggests that the exact MAP and MMSE estimates are not computable by the observer.

Nevertheless, we can approximate the prior distribution $p(\mathbf{w})$ from the sample statistics of \mathbf{w} . Notice that, 1) the parameter vector \mathbf{w} is a realization of the prior distribution $p(\mathbf{w})$; 2) once generated (after training), the parameter vector is determined and there is no randomness in \mathbf{w} . In this light, we will assume that the elements of \mathbf{w} are sampled from a generic Gaussian random variable W in an i.i.d. manner. In particular, the Gaussian is parameterized by the sample mean and sample variance of \mathbf{w} . Formally, we define a Gaussian random variable $W \sim \mathcal{N}(W; \mu_w, \sigma_w^2)$, where μ_w and σ_w^2 are the sample mean and sample variance of $\mathbf{w} = \{w[i] : i = 1, 2, \dots, d\}$. That is, $\mu_w = \frac{1}{d} \sum_{i=1}^d w[i]$ and $\sigma_w^2 = \frac{1}{d} \sum_{i=1}^d (w[i] - \mu_w)^2$.

Given this approximation, the elements of the observed sequence \mathbf{r} are also i.i.d., and can be viewed as realizations of a random variable $R = W + Z$, where $W \sim \mathcal{N}(W; \mu_w, \sigma_w^2)$ and $Z \sim \mathcal{N}(Z; 0, \sigma_z^2)$. Correspondingly, the MMSE and MAP estimates can be written as

$$\widehat{W}^{\text{MMSE}} \propto \min_{\widehat{W}} \int (\widehat{W} - W)^2 p(R|W) p(W) dW, \quad \widehat{W}^{\text{MAP}} \propto p(R|W) p(W). \quad (7)$$

The multiplication of two Gaussians is still a Gaussian, thus, $p(R, W) \propto p(R|W) p(W) \sim \mathcal{N}(W; \mu_p, \sigma_p^2)$, where $\mu_p = \frac{\sigma_w^2 R + \mu_w \sigma_z^2}{\sigma_w^2 + \sigma_z^2}$ and $\sigma_p^2 = \frac{\sigma_w^2 \sigma_z^2}{\sigma_w^2 + \sigma_z^2}$. As a result, the MMSE and MAP metrics are equivalent in that maximizing the posterior probability is equivalent to minimizing the MSE when the joint distribution $p(R, W)$ is Gaussian. We shall then focus on the MMSE estimate $\widehat{W}^{\text{MMSE}}$ below.

Following (7), the MSE between the estimated weight \widehat{W} and the true weight W can be written as

$$\text{MSE}_w = \mathbb{E} \left[(\widehat{W} - W)^2 | R \right] = \int (\widehat{W} - W)^2 p(W, R) dW. \quad (8)$$

Differentiating MSE_w with respect to \widehat{W} gives us

$$\frac{\partial \text{MSE}_w}{\partial \widehat{W}} = \int (\widehat{W} - W) p(W, R) dW = 0, \quad \widehat{W} = \int W p(W, R) dW = \mu_p.$$

We then arrive at the following MMSE estimator.

Definition 2 (MMSE estimation). *Given the observed NN weight vector $\mathbf{r} \in \mathbb{R}^d$ in (2), an MMSE estimator estimates the uncontaminated weight vector \mathbf{w} by*

$$\widehat{\mathbf{w}}^{MMSE} = \frac{\sigma_w^2}{\sigma_w^2 + \sigma_z^2} \mathbf{r} + \frac{\mu_w \sigma_z^2}{\sigma_w^2 + \sigma_z^2} \approx \frac{\sigma_w^2}{\sigma_w^2 + \sigma_z^2} \mathbf{r}, \quad (9)$$

where the approximation follows because the sample mean of the NN parameters is usually very small and can be ignored. The MMSE estimate in (9) is also the MAP estimate.

The MMSE estimator in (9) minimizes the MSE between $\widehat{\mathbf{w}}$ and \mathbf{w} . However, the ultimate goal of DL is not to minimize the MSE of the estimated weights, but to minimize the loss function $\mathcal{L}(\{\mathbf{x}^n, \mathbf{y}^n\}, \mathbf{w})$ between the NN output and the labels. Let $\mathcal{L}(\{\mathbf{x}^n, \mathbf{y}^n\}, \mathbf{w})$ be the MSE loss, for example, the ultimate goal is then to minimize the $MSE_{\mathcal{F}}$ given by

$$MSE_{\mathcal{F}} = \frac{1}{N} (\mathcal{F}(\mathbf{x}^n | \widehat{\mathbf{w}}) - \mathbf{y}^n)^\top (\mathcal{F}(\mathbf{x}^n | \widehat{\mathbf{w}}) - \mathbf{y}^n).$$

Said in another way, the MMSE estimator in (9), which minimizes MSE_w , does not necessarily minimize $MSE_{\mathcal{F}}$.

Analytically deriving the optimal estimate $\widehat{\mathbf{w}}$ that minimizes $MSE_{\mathcal{F}}$ is a non-trivial task in DL due to the non-linearity of the NN \mathcal{F} . In this context, we resort to empirical approaches in the next subsection and exploit two heuristics to revise the MMSE criterion in (7).

3.3 Bayesian estimation with compensators

We have two empirical observations: 1) in a NN, most of the parameter values are very small in magnitude; and 2) as far as the inference accuracy is concerned, the parameters with a larger magnitude matter more than those with a smaller magnitude. If we examine the MSE metric in (8), however, each parameter contributes equally to MSE_w regardless of its magnitude. This implies that the MMSE criterion and our ultimate goal of improving the inference accuracy are mismatched.

Considering that there is a large population of parameters that are very small in magnitude, we should add a population compensator to the MSE metric so that the estimation error of larger parameters (larger in magnitude) weighs more than the estimation error of smaller parameters. Specifically, instead of minimizing MSE_w , we propose to minimize MSE_p given by

$$MSE_p = \mathbb{E} \left[\left(\widehat{W} - W \right)^2 e^{\lambda W^2} | R \right] = \int \left(\widehat{W} - W \right)^2 e^{\lambda W^2} p(W, R) dW, \quad (10)$$

where λ is a temperature parameter that controls the extent to which we compensate for the smaller populations of larger parameters.

Given the new MSE_p metric, an $MMSE_p$ estimator can be derived as follows. Let $q_\lambda(W, R) = e^{\lambda W^2} p(W, R)$. Since $p(W, R) \sim \mathcal{N}(W; \mu_p, \sigma_p^2)$, we have

$$q_\lambda(W, R) \propto e^{\lambda W^2} e^{-\frac{(W - \mu_p)^2}{2\sigma_p^2}} \propto e^{-\frac{(W - \mu_\lambda)^2}{2\sigma_\lambda^2}},$$

where

$$\mu_\lambda = \frac{\mu_p}{1 - 2\sigma_p^2 \lambda} = \frac{\sigma_w^2 R}{\sigma_w^2 + (1 - 2\sigma_w^2 \lambda) \sigma_z^2}, \quad \sigma_\lambda^2 = \frac{\sigma_p^2}{1 - 2\sigma_p^2 \lambda} = \frac{\sigma_w^2 \sigma_z^2}{\sigma_w^2 + (1 - 2\sigma_w^2 \lambda) \sigma_z^2}.$$

In other words, $q_\lambda(W, R)$ is also Gaussian:

$$q_\lambda(W, R) \sim \mathcal{N}(W; \mu_\lambda, \sigma_\lambda^2). \quad (11)$$

In particular, to ensure that $\sigma_\lambda^2 > 0$, we impose $\lambda < \frac{1}{2\sigma_w^2} + \frac{1}{2\sigma_z^2}$.

Substituting (11) into (10) suggests that minimizing MSE_p is equivalent to minimizing MSE_w with a modified prior Gaussian with mean μ_λ and variance σ_λ^2 (as opposed to μ_p and σ_p^2). Following (8), the estimate W that minimizes MSE_p is then

$$\widehat{W} = \int W q_\lambda(W, R) dW = \mu_\lambda.$$

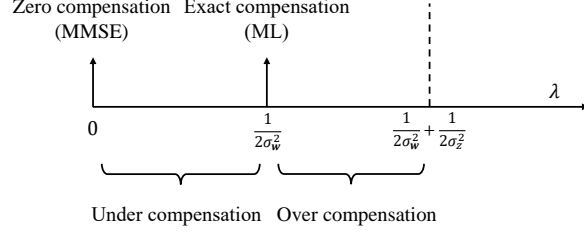


Figure 2: Relations among the ML, MMSE, and MMSE_p estimators.

Definition 3 (MMSE_p estimation). *Given the observed NN weight vector $\mathbf{r} \in \mathbb{R}^d$ in (2), an MMSE_p estimator estimates the uncontaminated weight vector \mathbf{w} by*

$$\hat{\mathbf{w}}^{\text{MMSE}_p} = \frac{\eta}{\eta + (1 - 2\sigma_w^2\lambda)} \mathbf{r}, \quad (12)$$

where $\eta = \sigma_w^2/\sigma_z^2$ is the received SNR and the temperature parameter $0 \leq \lambda < \frac{1}{2\sigma_w^2} + \frac{1}{2\sigma_z^2}$.

A comparison among the ML, MMSE, and MMSE_p estimators is illustrated in Fig. 2. As can be seen, for the MMSE_p estimator, the extent to which the population is compensated is controlled by the temperature parameter λ . For different values of λ , the ML and MMSE estimators can be viewed as special cases of the MMSE_p estimator. Specifically,

1. When $\lambda = 0$, we have $\hat{\mathbf{w}}^{\text{MMSE}_p} = \hat{\mathbf{w}}^{\text{MMSE}}$, and the MMSE_p estimator reduces to the MMSE estimator. We call it the zero-compensation point. For this setting, the contribution to the MSE of a parametric value $w[i]$ is proportional to $p(W)$ (see (7)). Thus, the more likely $w[i]$ is, the more the corresponding estimation error counts toward the MSE. Given that small weights are more likely, this setting may over-value the importance of small weights toward our learning algorithm.
2. When $\lambda = \frac{1}{2\sigma_w^2}$, we have $\hat{\mathbf{w}}^{\text{MMSE}_p} = \hat{\mathbf{w}}^{\text{ML}}$, the MMSE_p estimator reduces to the ML estimator. We call it the exact-compensation point. In this setting, $p(W)$ does not count. All values of w count equally toward the MSE regardless of the relative populations of different $w[i]$ as indicated in $p(W)$. Thus, the population bias in $p(W)$ is compensated away exactly.
3. When $0 < \lambda < \frac{1}{2\sigma_w^2}$, we call it the under-compensation region.
4. When $\frac{1}{2\sigma_w^2} < \lambda < \frac{1}{2\sigma_w^2} + \frac{1}{2\sigma_z^2}$, we call it the over-compensation region.

In addition to the population compensator, we empirically find that adding an extra compensation term, called the bias compensator, further improves the estimation performance. With the bias compensator, our goal is to minimize

$$\text{MSE}_{pb} = \mathbb{E} \left[\left(\widehat{W} - W \right)^2 e^{\lambda W^2 + \beta W} | R \right] = \int \left(\widehat{W} - W \right)^2 e^{\lambda W^2 + \beta W} p(W, R) dW, \quad (13)$$

where β is another temperature parameter to be tuned.

We next derive the MMSE_{pb} estimator that minimizes MSE_{pb} . Let $q_{\lambda,\beta}(W, R) = e^{\lambda W^2 + \beta W} p(W, R)$. Since $p(W, R) \sim \mathcal{N}(W; \mu_p, \sigma_p^2)$, we have

$$q_{\lambda,\beta}(W, R) \sim \mathcal{N}(W; \mu_{\lambda,\beta}, \sigma_{\lambda,\beta}^2), \quad (14)$$

where

$$\mu_{\lambda,\beta} = \frac{\mu_p + \sigma_p^2 \beta}{1 - 2\sigma_p^2 \lambda} = \frac{\sigma_w^2 R + \sigma_w^2 \sigma_z^2 \beta}{\sigma_w^2 + (1 - 2\sigma_w^2 \lambda) \sigma_z^2}, \quad \sigma_{\lambda,\beta}^2 = \frac{\sigma_p^2}{1 - 2\sigma_p^2 \lambda} = \frac{\sigma_w^2 \sigma_z^2}{\sigma_w^2 + (1 - 2\sigma_w^2 \lambda) \sigma_z^2}.$$

As can be seen, the bias compensator does not change the variance, i.e., $\sigma_{\lambda,\beta}^2 = \sigma_\lambda^2$. To ensure that $\sigma_{\lambda,\beta}^2 > 0$, the constraint is still $\lambda < \frac{1}{2\sigma_w^2} + \frac{1}{2\sigma_z^2}$.

Table 1: Test accuracies achieved by different NN models on the CIFAR-10 and SST-2 datasets.

Neural networks	ResNet34 (CIFAR-10)	ResNet18 (CIFAR-10)	ShuffleNet V2 (CIFAR-10)	BERT (SST-2)
#parameters	21.3M	11.2M	1.25M	109.5M
Test accuracy (centralized and noiseless)	95.81%	95.35%	92.12%	92.70%

Definition 4 (MMSE_{pb} estimation). *Given the observed NN weight vector $\mathbf{r} \in \mathbb{R}^d$ in (2), an MMSE_{pb} estimator estimates the uncontaminated weight vector \mathbf{w} by*

$$\hat{\mathbf{w}}^{MMSE_{pb}} = \frac{\eta}{\eta + (1 - 2\sigma_w^2\lambda)} \mathbf{r} + \frac{\sigma_w^2\beta}{\eta + (1 - 2\sigma_w^2\lambda)}, \quad (15)$$

where $\eta = \sigma_w^2/\sigma_z^2$ is the received SNR and $0 \leq \lambda < \frac{1}{2\sigma_w^2} + \frac{1}{2\sigma_z^2}$.

4 Experiments

In this section, we verify the performance of the MMSE_{pb} estimator benchmarked against the ML estimator via extensive experimental results. We shall focus on the CIFAR-10 image classification task and the SST-2 sentiment classification task, and implement different NN architectures to study NoisyNN under various SNRs. Due to the page limit, we report our main results in this section. More experimental details can be found in Appendices A and B.

Noisy inference: In the first part, we consider a class of NoisyNNs where noise is introduced only in the inference phase – the training phase is the standard centralized and noiseless training via backpropagation. For benchmarking purposes, we train three NN models (a ResNet34, a ResNet18, and a ShuffleNet V2) on the CIFAR-10 dataset, and a BERT model [25] on the SST-2 dataset in a noiseless and centralized manner. After training, the test accuracies (i.e., the prediction accuracy of the learned model on the test set) achieved by the four NN models on their respective test datasets are 95.81%, 95.35%, 92.12%, and 92.70%, respectively, as shown in Table 1.

For each well-trained NN, we add AWGN to the NN weights according to a given SNR η (in dB), and use the MMSE_{pb} and ML estimators to denoise the noisy weights. The denoised models are then evaluated on the test dataset to obtain test accuracies as the performance indicator of the estimators.

Fig. 3 presents the test accuracies achieved by different denoised models under various SNRs. In particular, we plot the average test accuracies as the solid curves and the standard deviations of the achieved test accuracies as shaded areas around the average test accuracies. For the experiments on the CIFAR-10 dataset, the average gains of the MMSE_{pb} estimator over the ML estimator are up to 156%, 85%, and 21% with the ResNet34, ResNet18, and ShuffleNet V2, respectively. In general, the MMSE_{pb} estimator exhibits larger gains over the ML estimator in larger networks. For the experiments on the SST-2 dataset, the MMSE_{pb} estimator improves the test accuracy of the denoised BERT model by up to 14.7% compared with the ML estimator.

Noisy training: In the first part, noise is introduced only in the inference phase on the already-trained NNs. In the second part, we investigate noisy training where noise is also introduced in the training phase. Specifically, we consider the application of FEEL with OAC: NNs are trained from scratch in a distributed manner over many iterations. In each iteration, AWGN is introduced in the uplink model aggregation step and we perform MMSE_{pb} estimation at the BS to estimate the aggregated model.

We implement a FEEL system wherein 20 edge devices collaboratively train a shared model. In particular, we focus on the CIFAR-10 task and consider two lightweight NNs, i.e., the ShuffleNet V2 and ResNet18, that are more suitable for mobile deployments. The training examples are assigned to the devices in a non-iid manner. For benchmark purposes, we train the two NN models in a FEEL and noiseless manner (i.e., the conventional federated learning setup [4]). With the non-iid assignment of training examples, the test accuracies of the ShuffleNet V2 and ResNet18 models are 83.01% and 89.52% when there is no AWGN noise.

Fig. 4 presents the test accuracies achieved by the learned models with the FEEL algorithm under various SNRs. As can be seen, for the ShuffleNet V2 model, the gains of the MMSE_{pb} estimator over

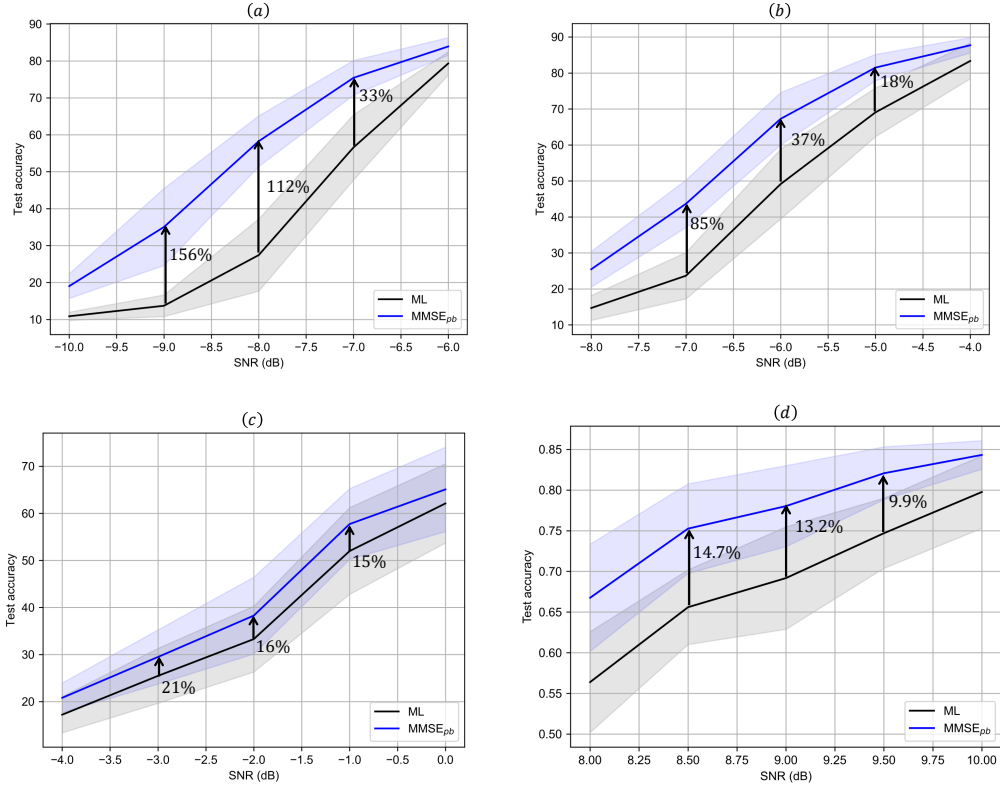


Figure 3: The average test accuracies of the estimated models on the CIFAR-10 and SST-2 datasets with the MMSE_{pb} estimator: (a) RestNet34 (CIFAR-10); (b) RestNet18 (CIFAR-10); (c) ShuffleNet V2 (CIFAR-10); (d) BERT (SST-2).

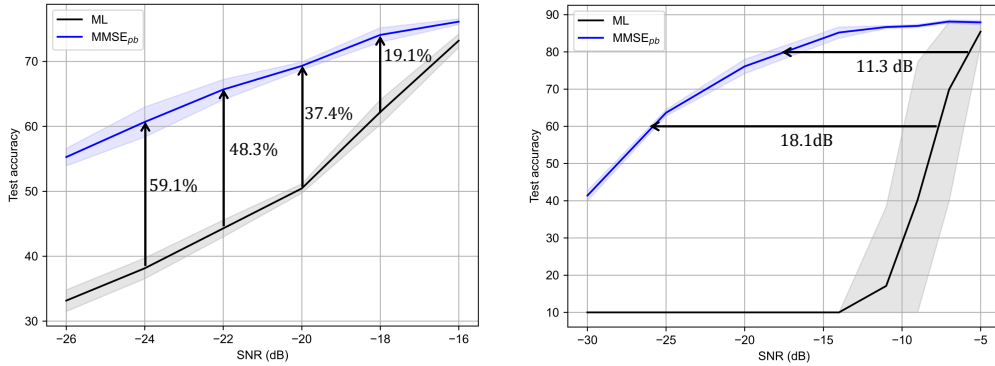


Figure 4: The average test accuracies of the learned NN models (ShuffleNet V2 on the LHS and ResNet18 on the RHS) in FEEL with the MMSE_{pb} estimator and the ML estimator.

the ML estimator are up to 59.1%. When it comes to ResNet18, the gains boost significantly. To achieve a test accuracy of 60%, the MMSE_{pb} estimator outperforms the ML estimator by 18.1 dB. On the other hand, to achieve a test accuracy of 80%, the MMSE_{pb} estimator outperforms the ML estimator by 11.3 dB.

Remark 2 (Limitation of our approach). *A main limitation of our approach is the lack of a method to determine the optimal temperature parameters λ and β before training and testing on a dataset. For all the experiments in this section, we identify the best temperature parameters by means of a grid search on the test dataset (see Appendix B). In doing so, we are able to present the best performance of the MMSE_{pb} estimator. This approach, however, may not be viable in practice due to the absence*

of “labels” for the test data. In Appendix B, we suggest two methods use in practice to find the temperature parameters for noisy inference and noisy training, respectively.

5 Conclusion

NoisyNN is a class of NNs whose weights are contaminated by noise. This paper puts forth an MMSE_{pb} estimator to estimate the uncontaminated NN weights from their noisy counterparts by exploiting the statistical characteristics of the NN weights. Unlike the widely-used ML estimator that maximizes the likelihood function of the estimated NN weights, our approach aims to minimize a compensated MSE of the estimated NN weights. Specifically, the compensated MSE is an MSE modified by a population compensator and a bias compensator. This formulation leads to a simple and efficient MMSE_{pb} estimator with significantly better empirical performance than the ML estimator, especially for large NN models. Our approach works well for NoisyNNs arising from both noisy training and noisy inference. Importantly, our work points out that focusing on minimizing the raw errors of the NN weights may not align perfectly with superior NN functional performance. We speculate that a fundamental reason could be that the weight errors affect the NN performance in a nonlinear way due to the nonlinear activation functions within the NN. Capturing the exact mechanic through which the weight errors affect the activations in NN awaits further investigation.

References

- [1] Guangxu Zhu, Yong Wang, and Kaibin Huang. Broadband analog aggregation for low-latency federated edge learning. *IEEE Trans. Wireless Commun.*, 19(1):491–506, 2019.
- [2] Mohammad Mohammadi Amiri and Deniz Gündüz. Machine learning at the wireless edge: Distributed stochastic gradient descent over-the-air. *IEEE Trans. Signal Process.*, 68:2155–2169, 2020.
- [3] Kai Yang, Tao Jiang, Yuanming Shi, and Zhi Ding. Federated learning via over-the-air computation. *IEEE Trans. Wireless Commun.*, 19(3):2022–2035, 2020.
- [4] Brendan McMahan, Eider Moore, Daniel Ramage, Seth Hampson, and Blaise Aguera y Arcas. Communication-efficient learning of deep networks from decentralized data. In *AI Statistics*, pages 1273–1282. PMLR, 2017.
- [5] D. Gündüz, D. B. Kurka, M. Jankowski, M. M. Amiri, E. Ozfatura, and S. Sreekumar. Communicate to learn at the edge. *IEEE Commun. Magazine*, 58(12):14–19, 2020.
- [6] Vinay Joshi, Manuel Le Gallo, Simon Haefeli, Irem Boybat, Sasidharan Rajalekshmi Nandakumar, Christophe Piveteau, Martino Dazzi, Bipin Rajendran, Abu Sebastian, and Evangelos Eleftheriou. Accurate deep neural network inference using computational phase-change memory. *Nature Commun.*, 11(1):1–13, 2020.
- [7] Stefano Ambrogio, Pritish Narayanan, Hsinyu Tsai, Robert M Shelby, Irem Boybat, Carmelo Di Nolfo, Severin Sidler, Massimo Giordano, Martina Bordini, Nathan CP Farinha, et al. Equivalent-accuracy accelerated neural-network training using analogue memory. *Nature*, 558(7708):60–67, 2018.
- [8] Chuteng Zhou, Prad Kadambi, Matthew Mattina, and Paul N Whatmough. Noisy machines: Understanding noisy neural networks and enhancing robustness to analog hardware errors using distillation. *arXiv preprint arXiv:2001.04974*, 2020.
- [9] Jonathan Binas, Daniel Neil, Giacomo Indiveri, Shih-Chii Liu, and Michael Pfeiffer. Precise deep neural network computation on imprecise low-power analog hardware. *arXiv: 1606.07786*, 2016.
- [10] Yichen Shen, Nicholas C Harris, Scott Skirlo, Mihika Prabhu, Tom Baehr-Jones, Michael Hochberg, Xin Sun, Shijie Zhao, Hugo Larochelle, Dirk Englund, et al. Deep learning with coherent nanophotonic circuits. *Nature Photonics*, 11(7):441, 2017.

- [11] Berivan Isik, Kristy Choi, Xin Zheng, Tsachy Weissman, Stefano Ermon, H-S Philip Wong, and Armin Alaghi. Neural network compression for noisy storage devices. *arXiv preprint arXiv:2102.07725*, 2021.
- [12] R.M. Gray and D.L. Neuhoff. Quantization. *IEEE Trans. Inf. Theory*, 44(6):2325–2383, 1998.
- [13] Léopold Cambier, Anahita Bhiwandiwala, Ting Gong, Mehran Nekuii, Oguz H Elibol, and Hanlin Tang. Shifted and squeezed 8-bit floating point format for low-precision training of deep neural networks. *arXiv:2001.05674*, 2020.
- [14] D.H. Lee and D.L. Neuhoff. Asymptotic distribution of the errors in scalar and vector quantizers. *IEEE Trans. Inf. Theory*, 42(2):446–460, 1996.
- [15] R. Zamir and M. Feder. On lattice quantization noise. *IEEE Trans. Inf. Theory*, 42(4):1152–1159, 1996.
- [16] Alon Kipnis and Galen Reeves. Gaussian approximation of quantization error for estimation from compressed data. In *IEEE Int. Symp. Inf. Theory (ISIT)*, 2019.
- [17] Mohammad Mohammadi Amiri, Tolga M. Duman, Deniz Gunduz, Sanjeev R. Kulkarni, and H. Vincent Poor. Blind federated edge learning. *arXiv cs.IT.2010.10030*, 2020.
- [18] G. Zhu, Y. Du, D. Gunduz, and K. Huang. One-bit over-the-air aggregation for communication-efficient federated edge learning: Design and convergence analysis. *IEEE Trans. Wireless Commun.*, 2020.
- [19] Yulin Shao, Deniz Gündüz, and Soung Chang Liew. Federated learning with misaligned over-the-air computation. *Technical report, available online: <https://arxiv.org/abs/2009.13441>*, 2021.
- [20] Omobayode Fagbohunbe and Lijun Qian. Benchmarking inference performance of deep learning models on analog devices. *arXiv preprint arXiv:2011.11840*, 2020.
- [21] Alex Krizhevsky, Geoffrey Hinton, et al. Learning multiple layers of features from tiny images. *Technical report*, 2009.
- [22] Richard Socher, Alex Perelygin, Jean Wu, Jason Chuang, Christopher D Manning, Andrew Y Ng, and Christopher Potts. Recursive deep models for semantic compositionality over a sentiment treebank. In *EMNLP*, pages 1631–1642, 2013.
- [23] Kaiming He, Xiangyu Zhang, Shaoqing Ren, and Jian Sun. Deep residual learning for image recognition. In *IEEE CVPR*, pages 770–778, 2016.
- [24] Ningning Ma, Xiangyu Zhang, Hai-Tao Zheng, and Jian Sun. Shufflenet v2: practical guidelines for efficient cnn architecture design. In *ECCV*, pages 116–131, 2018.
- [25] Jacob Devlin, Ming-Wei Chang, Kenton Lee, and Kristina Toutanova. Bert: pre-training of deep bidirectional transformers for language understanding. *arXiv:1810.04805*, 2018.
- [26] Meire Fortunato, Mohammad Gheshlaghi Azar, Bilal Piot, Jacob Menick, Ian Osband, Alex Graves, Vlad Mnih, Remi Munos, Demis Hassabis, Olivier Pietquin, et al. Noisy networks for exploration. *arXiv preprint arXiv:1706.10295*, 2017.
- [27] Guozhong An. The effects of adding noise during backpropagation training on a generalization performance. *Neural computation*, 8(3):643–674, 1996.
- [28] Yulin Shao, Soung Chang Liew, and Deniz Gündüz. Denoising noisy neural networks: a Bayesian approach with compensation. *Source code, online: <https://github.com/lynshao/NoisyNN>*, 2021.

A Implementation Details

A.1 Datasets and neural networks

The results in Section 4 are based on extensive experiments on two classical datasets: CIFAR-10 [21] and SST-2 [22]. The experiments were conducted on a Linux server with two CPU (Intel Xeon E5-2643) and four GPUs (GeForce GTX 1080Ti).

The CIFAR-10 dataset (MIT license) consists of 60,000 32×32 colour images in 10 classes, with 6,000 images per class. There are 50,000 training images and 10,000 test images. The NNs used are ResNet34, ResNet18, and ShuffleNet V2. Their detailed architectures can be found in [23] and [24], respectively.

The SST-2 dataset (GNU general public license) is a corpus with fully labeled parse trees that allows for a complete analysis of the compositional effects of sentiment in language. The corpus consists of 6,920 training examples and 1,821 test examples, where each example is labelled as either positive or negative. The NN used is a BERT model proposed in [25].

All our codes and data are available online at [28].

A.2 Noisy inference

In noisy inference, noise is introduced to already-trained NNs. Prior to that, the NNs were trained in a centralized and noiseless manner.

For the CIFAR-10 dataset, the training of ResNet34, ResNet18, and ShuffleNet V2 followed [R1] (MIT license). After training, the test accuracies achieved by the NN models were 95.81%, 95.35%, and 92.12%, respectively. For the SST-2 dataset, we first downloaded a pretrained BERT model from Hugging Face [R2] and then fine-tuned the pretrained model on the SST-2 dataset [R3]. The resulting BERT model achieved an accuracy of 92.70% on the test dataset.

We then added AWGN to the well-trained NN weights under a given SNR and used different estimators to denoise the noisy weights. A caveat here is that the parameters of the batch-normalization and the layer-normalization layers were set to be noise-free in the experiments [6, 8], because they behave differently than other parameters [20]. These parameters are few in number. In practice, we can transmit/store them in a reliable manner (for example, via digital communication/storage [6] or protect them by repetition coding [11]).

A.3 Noisy training

In noisy training, the NNs are trained from scratch with AWGN introduced in each training iterations. In the experiments, we considered the application of FEEL with OAC, where 20 edge devices collaboratively train a neural network to solve the CIFAR-10 task. The models we used are two lightweight NNs: ShuffleNet V2 and ResNet18.

Recall that the CIFAR-10 dataset has a training set of 50,000 examples and a test set of 10,000 examples in 10 classes. We assigned non-i.i.d. training examples to the 20 devices in the following manner: 1) first, we let each device randomly sample 2,000 samples from the training dataset; 2) for the remaining 10,000 examples in the training dataset, we sorted them by their labels and grouped them into 20 shards of size 500 [4]. Each device was then assigned one shard.

In each iteration, $M = 4$ devices actively participating in the training. Each device trains the global model locally for 5 epochs and transmits the model-update to the BS in each iteration [R4]. The PS then employs the ML and MMSE_{pb} estimators to denoise the received NN models.

[R1] K. Liu. Train CIFAR-10 with PyTorch. Available online: <https://github.com/kuangliu/pytorch-cifar>, MIT license, 2020.

[R2] Hugging Face. A pretrained BERT model with text attack. Available online: <https://huggingface.co/textattack/bert-base-uncased-SST-2>, 2021.

[R3] Y. Jiang. SST-2 sentiment analysis. Available online: <https://github.com/YJiangcm/SST-2-sentiment-analysis>, MIT license, 2020.

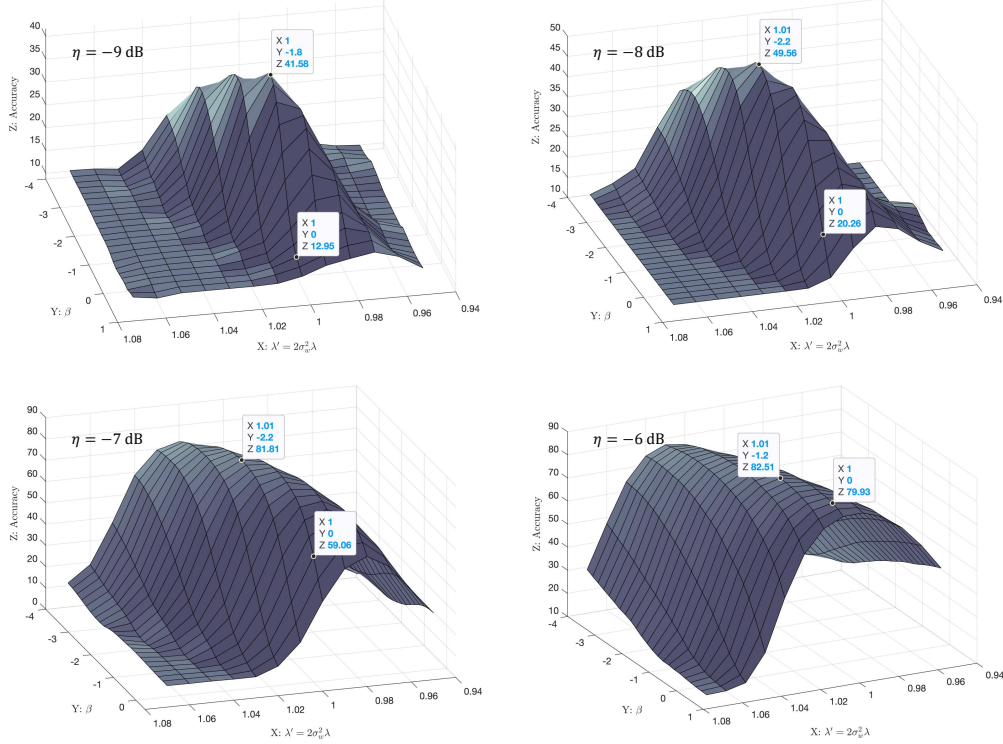


Figure 5: Test accuracy of the estimated model from a noisy ResNet34 using the MMSE_{pb} estimator under various temperature parameters λ' and β : the x-axis is $\lambda' = 2\sigma_w^2\lambda$ ($\sigma_w^2 = 2.6 \times 10^{-5}$), the y-axis is β , the z-axis is the test accuracy. Noise is added to the well-trained ResNet34 according to a given SNR η (in dB). When $\lambda' = 1$ and $\beta = 0$, the MMSE_{pb} estimator reduces to the ML estimator.

[R4] S. Ji. A PyTorch implementation of federated learning. Available online: <https://github.com/shaoxiongji/federated-learning>, MIT license, 2018.

B Temperature Parameters

There are four parameters to be determined in the MMSE_{pb} estimator: the sample variance of NN weights σ_w^2 , the noise variance σ_z^2 , and the temperature parameters λ and β . The first two parameters σ_w^2 and σ_z^2 are often readily available to an observer/receiver. For example, in the application of FEEL, the noise variance σ_z^2 can be estimated by the receiver when there is no signal transmission. The sample variance of NN weights σ_w^2 , on the other hand, can be estimated by the receiver from the sample variance of the observed vector, i.e., σ_r^2 , when there are signal transmissions. This is because

$$\mu_w = \mu_r, \quad \sigma_w^2 = \sigma_r^2 - \sigma_z^2,$$

where $\mu_r = \frac{1}{d} \sum_{i=1}^d r[i]$ and $\sigma_r^2 = \frac{1}{d} \sum_{i=1}^d (r[i] - \mu_r)^2$ can be obtained directly from the received or observed vector.

In comparison, determining the optimal temperature parameters λ and β is more intricate. In the experiments of Section 4, we identified the best temperature parameters by means of a grid search on the test dataset. In this way, we were able to present the best performance of the MMSE_{pb} estimator. In the following, we elaborate on how the grid search was performed.

To start with, we define a new temperature parameter $\lambda' = 2\sigma_w^2\lambda$ to replace λ . In all the experiments, we used a fixed λ' instead of a fixed λ . For noisy inference, σ_w^2 is a constant for a well-trained NN, and hence, a fixed λ' also means a fixed λ . For noisy training, however, σ_w^2 varies as training goes on – a fixed λ' indicates a variable λ over the course of training.

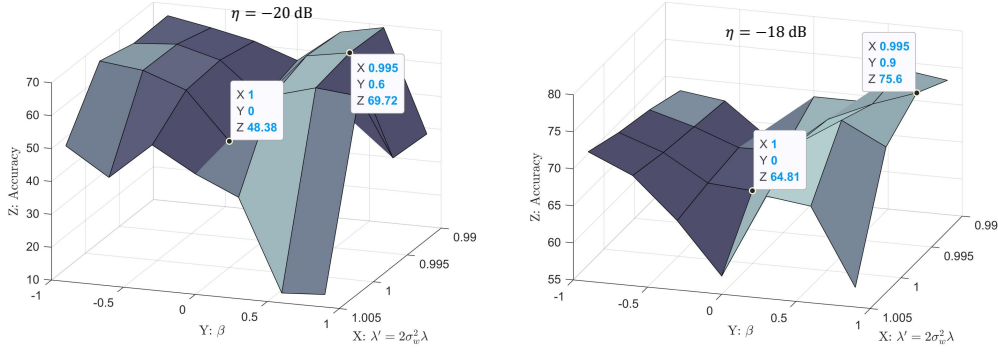


Figure 6: Test accuracies of the learned ShuffleNet V2 model with FEEL. The SNRs are -20 dB (left) and -18 dB (right), respectively. We use the MMSE_{pb} estimator at the BS with various combinations of $\lambda' = 2\sigma_w^2 \lambda$ and β . Note that λ' and β are fixed over the training iterations. When $\lambda' = 1$ and $\beta = 0$, the MMSE_{pb} estimator reduces to the ML estimator.

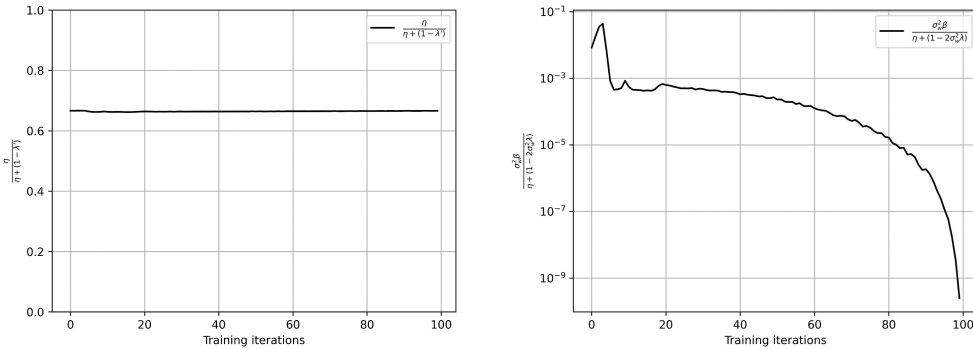


Figure 7: The evolutions of the multiplication factor $\frac{\eta}{\eta+(1-\lambda')}$ and the additive bias $\frac{\sigma_w^2 \beta}{\eta+(1-\lambda')}$ over the course of FEEL. The NN model is a ShuffleNet V2 network. The temperature parameters are fixed to $\lambda' = 2\sigma_w^2 \lambda = 0.995$ and $\beta = 0.6$.

Noisy inference: We focus on the experiments of ResNet34 for the CIFAR-10 task here. Fig. 5 presents the test accuracy of the denoised ResNet34 model with the MMSE_{pb} estimator, wherein each subfigure corresponds to the performance of the estimated model under a given SNR η , and we used various combinations of λ' and β to find the maximum test accuracy. Note that when $\lambda' = 1$ and $\beta = 0$, the MMSE_{pb} estimator reduces to the ML estimator. Running the experiments in Fig. 5 many times gave us the average performance in Fig. 3(a).

We have three observations from Fig. 5:

1. ML estimation is in general suboptimal. With properly chosen temperature parameters, the MMSE_{pb} estimator outperforms the ML estimator by a large margin, especially in the low-SNR regime.
2. The test-accuracy gains of the MMSE_{pb} estimator over the ML estimator decrease as the SNR increases. This is easy to understand since there is not much noise in the high SNR regime.
3. For different SNRs, the shapes of the surface plots are very similar, suggesting that we can use the same set of temperature parameters across various SNRs.

Noisy training: We focus on the ShuffleNet V2 model for the CIFAR-10 task. Fig. 6 presents the test accuracies achieved by the learned ShuffleNet V2 model with the FEEL algorithm. The SNRs are -20 dB (left) and -18 dB (right), respectively. The MMSE_{pb} estimator was used at the BS to estimate the aggregated model at each iteration. Running the experiments in Fig. 6 many times gave us the average performance in Fig. 4 (left).

To find the best performance of the MMSE_{pb} estimator, we performed a grid search by running the FEEL algorithm with various combinations of temperature parameters λ' and β . In particular, λ' and β were fixed in one run of FEEL. For example, when SNR is -20 dB, the best performance achieved by the MMSE_{pb} estimator is 69.72% when $\lambda' = 0.995$ and $\beta = 0.6$ (see Fig. 6 on the LHS). To obtain this performance, we ran the FEEL algorithm with fixed $\lambda' = 0.995$ and $\beta = 0.6$ over the course of training. Recall from (15) that the MMSE_{pb} estimator consists of a multiplication factor $\frac{\eta}{\eta+(1-\lambda')}$ and an additive bias term $\frac{\sigma_w^2\beta}{\eta+(1-\lambda')}$. Fig. 7 shows how the multiplication factor and the additive bias evolve over the course of FEEL: for fixed η , λ' , and β , the multiplication factor is a constant while the additive bias is proportional to the signal variance σ_w^2 .

For all experiments in this paper, we performed a grid search for the optimal temperature parameters on the test dataset and presented the best performance of the MMSE_{pb} estimator. It is worth noting that this approach is not viable in practice due to the absence of “labels” for the test data. Thus, we suggest the following methods to determine the temperature parameters in practice: 1) For noisy inference, the entity who trains the NNs can perform an additional grid search on the training dataset to find the best temperature parameters, by introducing simulated noise to the NN weights. The found temperature parameters are then transmitted/stored in a reliable way (using repetition code, for example) so that a receiver/retriever can use them to perform the MMSE_{pb} estimation. 2) For noisy training such as FEEL, often a small portion of data is available at the BS. The BS can use this data to find the best temperature parameters to denoise the NoisyNN.